

Dehydrocorydaline inhibits the tumorigenesis of breast cancer MDA-MB-231 cells

YING HUANG^{1*}, HUI HUANG^{1*}, SHIYING WANG², FEIXIANG CHEN³ and GANG ZHENG³

Departments of ¹Oncology, ²Anesthesiology and ³General Surgery, The Fifth Hospital of Wuhan, Wuhan, Hubei 430050, P.R. China

Received June 25, 2019; Accepted December 16, 2019

DOI: 10.3892/mmr.2020.11122

Abstract. Dehydrocorydaline (DHC) is an alkaloid isolated from *Corydali syanhusuo* that exhibits antitumor properties. It has been reported that DHC can inhibit the proliferation of breast cancer cells, however the underlying molecular mechanism remains elusive. Therefore, the main objective of this study was to evaluate the antitumor activity of DHC, and gain further insights into its mechanism of action. The viability of MDA-MB-231 cells was determined through a Cell Counting Kit-8 assay. The effect of DHC on the proliferation of MDA-MB-231 cells was detected by flow cytometry and 5-ethynyl-2'-deoxyuridine staining. Apoptosis was evaluated by Annexin V-FITC and PI staining through flow cytometry. The impact of DHC treatment on the colony-forming ability of breast cancer cells was assessed. The expression levels of proliferation-associated genes cyclin-dependent kinases 1 (*CDK1*) and cyclin D1 (*CCND1*) and apoptosis-related genes *BCL2* and *caspases 3/8/9* were quantified by real-time PCR. Western blot analysis was performed to evaluate the production of cleaved caspase 3/9 and matrix metalloproteinase (MMP)2/9. DHC-treated MDA-MB-231 cells were subcutaneously injected into mice. Subsequent immunohistochemical analyses were performed. DHC inhibited the viability, proliferation, colony-forming ability and migration of MDA-MB-231 cells; in addition, DHC treatment promoted their apoptosis. DHC inhibited the production of proliferation- and anti-apoptosis-associated proteins CDK1, CCND1, BCL2 as well as that of the

metastasis-associated proteins MMP2 and MMP9. However, it promoted the expression of the pro-apoptotic caspases 3/8/9. Moreover, DHC inhibited the growth of MDA-MB-231 tumor xenografts in SCID mice, and decreased cell proliferation in newly formed tumors *in vivo*. DHC exerted anticancer effects by downregulating cell proliferation, antiapoptosis, metastasis-associated proteins CDK1, CCND1, BCL2 and metastasis-associated proteins MMP2 and MMP9, and by upregulating the expression of proapoptotic proteins caspase 3/8/9.

Introduction

Female breast cancer is a major health problem that accounts for 30% of cancer cases worldwide; therefore, breast cancer is the most common type of cancer in women (1). The incidence of breast cancer varies greatly worldwide, with 0.194 in East Africa and 0.897 in Western Europe, exhibiting an overall increasing trend (2). Generally, breast cancer patients rely on conventionally available chemotherapy; however, the results are often unsatisfactory with a poor patient prognosis. There are many risk factors associated with breast cancer, including the use of hormonal contraceptives, sedentariness, and alcohol consumption; however, its etiology and pathogenesis are still not clearly understood. Therefore, there is an urgent need to develop new drugs to improve the prognosis of breast cancer patients.

Natural products provide a valuable source of anticancer compounds. Many commonly used chemotherapeutic drugs, such as vinblastine, etoposide, paclitaxel, and camptothecin, are derived directly or indirectly from natural products. Among the various plant bioactive compounds, alkaloids appear to have the most prominent anticancer effect. Camptothecin and vinblastine are two of the most notable examples (3), and other alkaloids, such as berberine and isoquinoline, also exhibit antitumor potential (4). Previous studies have reported that dehydrocorydaline (DHC), an alkaloid isolated from *Corydali syanhusuo* (WT Wang, 1985), presents anticancer potential. However, there are very few studies on the use of DHC for breast cancer treatment. Previous studies indicated that DHC exerts anti-allergic and antitumor effects, and can inhibit the proliferation of MCF-7 breast cancer cells *in vitro* (5). However, the underlying mechanism of action remains unclear.

Correspondence to: Dr Gang Zheng, Department of General Surgery, The Fifth Hospital of Wuhan, 122 Xianzheng Road, Wuhan, Hubei 430050, P.R. China
E-mail: zgengand12@163.com

*Contributed equally

Abbreviations: CDK1, cyclin-dependent kinases 1; CCND1, cyclin D1; MMP, matrix metalloproteinase; PCNA, proliferating cell nuclear antigen

Key words: breast cancer, apoptosis, cell proliferation, cell migration, natural products

Among the many metastasis-related molecules, CDK1, CCND1, and MMP family members are known to be closely related to cell proliferation, migration, and differentiation. In addition, the BCL2 and caspase family proteins are involved in apoptosis (6). These molecules may also play a key role in the inhibition of breast cancer mediated by DHC. In the present study, the effects of DHC treatment on cell proliferation and migration, as well as on the expression of apoptotic markers *in vitro* and *in vivo* were evaluated, thus revealing the molecular mechanism of DHC against cancer.

Materials and methods

Cell culture. For the present study, human breast cancer cells MDA-MB-231 were obtained from the American Type Culture Collection (ATCC). During the experimental protocol, cells were cultured in the Dulbecco's modified Eagle medium-high glucose (H-DMEM) supplemented with 10% fetal bovine serum (FBS), 100 U/ml penicillin, and 100 $\mu\text{g}/\text{ml}$ streptomycin (all from Gibco; Thermo Fisher Scientific, Inc.). Cells were maintained at 37°C in a humidified atmosphere supplemented with 5% CO₂ in an incubator. The culture medium was changed every ~2-3 days. Cells were passaged when the cell confluency reached ~80-90%; cells from different flasks were passaged independently.

Cell viability. The viability of MDA-MB-231 cells after treatment with DHC (dissolved in DMSO) was assessed through a Cell Counting Kit-8 (CCK-8) assay. After trypsinization (0.25%) at 37°C for 2 min, cells were seeded on 96-well plates at a cell density of 3x10⁴ cells/cm² and cultured for 24 h at 37°C, to allow adequate cell attachment. Then, the culture medium was replaced with FBS-free H-DMEM for cell starvation. After 24 h of starvation at 37°C, the medium was changed with fresh 10% FBS H-DMEM supplemented with various concentrations of DHC (20, 30, 40, 50 or 100 μM). In addition, the DMSO-treatment group was set as the blank group, and the non-treatment group was set as the control group. All cells were cultured for 48 or 72 h at 37°C, then cell viability was evaluated by a CCK-8 assay. A volume of 10 μl CCK-8 (Beijing Solarbio Science & Technology Co., Ltd.) was added in each well, and the plates were incubated for 1 h in the dark. Then, the absorbance was measured at 450 nm using a microplate spectrophotometer.

Cell proliferation. The effect of DHC treatment on the proliferation of MDA-MB-231 cells was evaluated by 5-ethynyl-2'-deoxyuridine (EdU) staining and flow cytometry. For EdU staining, cells were seeded on 96-well plates at a cell density of 3x10⁴ cells/cm². After starvation at 37°C overnight, the cells were treated with various concentrations of DHC (10, 50 or 100 μM) for 22 or 46 h at 37°C, and incubated with 50 μM EdU for another 2 h at 37°C. Subsequently, the samples were fixed with 4% paraformaldehyde at room temperature for 20 min. After 3x5 min washes with PBS, cells were stained with 100 μl Apollo 567 stain reaction buffer for 30 min at room temperature. Then, the cells were washed again with PBS, and stained with DAPI (5 $\mu\text{g}/\text{ml}$) at room temperature for 15 min. Finally, EdU-labelled cells were visualized under a fluorescence microscope (magnification, x200; five random

fields of view). Image-Pro Plus software (version 6.0; Media Cybernetics, Inc.) was used to quantify EdU-labelled cells. The ratio of EdU-positive cells was calculated using the following formula: EdU add-in cells/DAPI-stained cells x100%. For the flow cytometric assay, MDA-MB-231 cells were treated with 100 μM DHC for 48 h at 37°C. Then, cells were washed once with pre-cooled PBS and centrifuged (300 x g for 5 min at 4°C). Cells were fixed with 500 μl 70% ethanol at 4°C for 2 h. After fixation, the cells were washed once with PBS, and the cell suspension was incubated with 100 μl RNase A at 37°C for 30 min. Propidium iodide (PI; 400 μl ; cat. no. C0080; Solarbio biotech, Beijing, cat. no. C0080) was added into the cell suspension, which was then incubated at 4°C for 30 min in the dark. Samples were analyzed using a BD FACSCalibur flow cytometer (BD Biosciences) at 488 nm excitation wavelength and FlowJo software (version 7.6.1; Tree Star, Inc.).

Cell apoptosis. In the present study, cell apoptosis was evaluated by Annexin V-FITC and PI staining and flow cytometry. In brief, MDA-MB-231 cells were seeded on 6-well plates and treated as described in the previous sections. After cell starvation, 50 μM DHC was added into the culture medium, and the cells were cultured for another 48 h at 37°C. Subsequently, the apoptosis of MDA-MB-231 cells was evaluated using an Annexin V-FITC/PI kit (cat. no. FAK012; Neobioscience), according to the manufacturer's protocol. Cells were washed twice in PBS by centrifugation (300 x g for 5 min at 4°C), and resuspended in 195 μl binding buffer. Subsequently, 5 μl Annexin V-FITC and 10 μl PI were added to each cell suspension and incubated for 10 min at RT in the dark. The samples were analyzed using a BD FACSCalibur flow cytometer (BD Biosciences) and FlowJo software (version 7.6.1; Tree Star, Inc.).

Colony formation. Alterations in the colony-forming activity of MDA-MB-231 cells after treatment with DHC were also evaluated. MDA-MB-231 cells were seeded on 6-well plates at a cell density of 1x10³ cells/well. Subsequently, 50 or 100 μM DHC were added into the culture medium, and the cells were cultured for 12 days at 37°C. The medium was changed every 3 days. Then, the cells were stained using crystal violet solution (cat. C8470; Beijing Solarbio Science & Technology, Co., Ltd.) at room temperature for 15 min, images were captured, and colonies with >50 cells were counted using a light microscope (magnification, x100).

Scratch assay. The invasive capacity of the MDA-MB-231 cells was verified through a scratch assay. MDA-MB-231 cells were seeded on 6-well plates at a cell density of 3x10⁴ cells/cm². When the cells reached confluence, a line of 10x1.4 mm (length x width) was created by scraping the cells with a pipette tip. Then, the suspended cells were washed away, and 2% FBS H-DMEM was added into the wells. After another 48 h at 37°C, the migrated cells were imaged and counted using a light microscope (magnification, x100).

Reverse transcription-quantitative PCR (RT-qPCR). Based on the aforementioned experiments, only the effects of treatments with 20 and 50 μM DHC on the expression level of various genes were verified. The expression levels of

Table I. Primers used for reverse transcription-quantitative PCR.

| Gene | Sequence (5'→3') | |
|-------|-------------------------------|-----------------------------|
| | Forward | Reverse |
| CDK1 | 5'-CTGGCTCTTGAAATTGAGCG-3' | 5'-CTGGCAAGGCCAAAATCAGC-3' |
| CCND1 | 5'-CTGATTGGACAGGCATGGGT-3' | 5'-GTGCTGGAAGTCAACGGTA-3' |
| BCL2 | 5'-GGTGGGGTCATGTGTGTGG-3' | 5'-CGGTCAGGTACTCAGTCATCC-3' |
| CASP3 | 5'-CATGGAAGCGAATCAATGGACT-3' | 5'-CTGTACCAGACCGAGATGTCA-3' |
| CASP8 | 5'-CGGACTCTCCAAGAGAACAGG-3' | 5'-TCAAAGGTCGTGGTCAAAGCC-3' |
| CASP9 | 5'-CTTCGTTTCTGCGAACTAACAGG-3' | 5'-GCACCACTGGGGTAAGGTTT-3' |
| GAPDH | 5'-GCACCGTCAAGGCTGAGAAC-3' | 5'-TGGTGAAGACGCCAGTGGA-3' |

CDK1, cyclin-dependent kinases 1; CCND1, cyclin D1; CASP, caspase.

proliferation-associated genes (*CDK1* and *CCND1*) and apoptosis-relevant genes (*BCL2*, *caspases 3/8/9*) were assessed by RT-qPCR. Total RNA was extracted using the RNA simple total RNA kit (Tiangen Biotech Co., Ltd.), according to the manufacturer's instructions, from both the control and experimental groups (cells treated with DHC for 48 h). Subsequently, isolated mRNA was reverse-transcribed to cDNA using the RevertAid™ First Strand cDNA synthesis kit (Thermo Fisher Scientific, Inc.), according to the manufacturer's protocol. The mRNA expression levels of the aforementioned genes and *GAPDH* were quantified. qPCR was performed on the Bio-rad CFX96™ Real-Time PCR system (Bio-Rad Laboratories, Inc.) using the PCR Master Mix kit (Promega Corporation), according to the manufacturer's protocol. The primer pairs used for qPCR are listed in Table I. The following thermocycling conditions were used for qPCR: Initial denaturation at 95°C for 30 sec; followed by 39 cycles of 95°C for 5 sec and 60°C for 30 sec; and a final extension at 72°C for 5 min. mRNA levels were quantified using the $2^{-\Delta\Delta C_t}$ method (7) and normalized to the internal reference gene *GAPDH*.

Western blotting. Western blotting was performed to quantify the protein expression levels of cleaved caspase 3/9 and MMP2/9. After 48 h of DHC treatment, cells were harvested and lysed in RIPA buffer (Beyotime Institute of Biotechnology) supplemented with protease inhibitors to extract total protein. Total protein was quantified using a bicinchoninic acid assay. Subsequently, 35 µg protein/lane were separated by SDS-PAGE on 10% polyacrylamide gels and transferred to PVDF membranes. Subsequently, the membranes were blocked with Tris-buffered saline (TBS) containing 5% non-fat dry milk at 37°C for 30 min. The membranes were incubated overnight at 4°C with primary antibodies targeted against: MMP2 (cat. no. ab92536; 1:1,000; Abcam), MMP9 (cat. no. ab76003; 1:1,000; Abcam), cleaved caspase 3 (cat. no. ab2302; 1:1,000; Abcam), cleaved caspase 9 (cat. no. ab185719; 1:1,000; Abcam) and *GAPDH* (cat. no. 10494-1-AP; 1:5,000; ProteinTech Group, Inc.). Following primary incubation, the membranes were incubated with a secondary antibody (cat. no. ab6721; 1:5,000; Abcam) at 37°C for 1 h. Finally, the immunoreactive bands were developed using the Supersignal West Femto Maximum

Sensitivity Substrate (Thermo Fisher Scientific, Inc.), and the corresponding images were analyzed using the Quantity One Software (version 4.6.6; Bio-Rad Laboratories, Inc.) using *GAPDH* as the loading control.

Animal experiments. In the present study, 8 female SCID mice (age, 6-8 weeks; weight, 20 g) were kept in pathogen-free conditions at 25°C with 12-h light dark cycles and access to food and water *ad libitum*. Mice were randomly divided into two groups (control and experimental). In the control group, MDA-MB-231 cells (3×10^6 cells resuspended in 100 µl Matrigel) were injected subcutaneously into both flanks of each mouse. In the experimental group, after subcutaneous implantation of MDA-MB-231 cells, 500 µM DHC (50 µl) was injected locally daily during the first 3 days, and every other day for the next 10 days. The animals were euthanized by CO₂ inhalation until they ceased breathing completely and then cervical dislocation followed. The tumor weight was measured 2 weeks after the implantation of breast cancer cells. The tumors were snap-frozen in liquid nitrogen and submitted for immunohistochemical (IHC) analyses. All the animal experiments were carried out according to ethical principles and protocols approved by the Fifth Hospital of Wuhan.

IHC analyses. All tumor samples were fixed in 4% paraformaldehyde at 4°C overnight and washed with PBS later. The samples were dehydrated, embedded in paraffin, and cut into 5 µm-thick sections using a cryostat. H&E (Beijing Solarbio Science & Technology Co., Ltd.) staining was performed on the sections, according to the manufacturer's protocol. Protein expression levels of Ki67, proliferating cell nuclear antigen (PCNA) were verified through immunofluorescence (IF) staining. Firstly, antigen retrieval was performed by incubation in 0.01 M sodium citrate buffer solution (pH=6.0) for 25 min in a water bath at 95°C. Sections were incubated with primary antibodies against Ki67 (cat. no. ab16667; 1:100; Abcam), PCNA (cat. no. ab92552; 1:100; Abcam) at 4°C overnight. Subsequently, the sections were incubated with an Alexa Fluor 488-conjugated secondary antibody (cat. no. A32731; 1:1,000; Thermo Fisher Scientific, Inc.) for 1 h at room temperature. Nuclei were stained with DAPI for 10 min at room temperature. Cell proliferation and

histological alterations in the DHC group compared with the control were examined by fluorescence microscopy (magnification, x200; five random fields of view). The images were analyzed using Image-Pro Plus software (version 6.0; Media Cybernetics, Inc.).

Statistical analyses. All experiments were performed at least four times. Data are presented as the mean \pm SD. Statistical analysis was performed using one-way ANOVA followed by Tukey's post hoc test. Statistical analyses were performed using Origin software (version 8.0; OriginLab). $P < 0.05$ was considered to indicate a statistically significant difference.

Results

DHC inhibits the viability of MDA-MB-231 cells. After treatment with various concentrations of DHC, the viability of MDA-MB-231 cells decreased in a dose-dependent manner. As revealed in the Fig. 1, DMSO exerted no evident effect on the viability of MDA-MB-231 cells; cell viability was significantly decreased after treatment with increasing concentrations of DHC. At 24 h, 20, 30, 40, 50, and 100 μM DHC decreased the viability of MDA-MB-231 cells from 101.02 ± 9.04 to 61.24 ± 8.62 , 42.77 ± 9.74 , 40.13 ± 5.37 , 32.45 ± 2.62 , and 36.03 ± 7.13 , respectively (Fig. 1, upper image). Moreover, treatment with 20, 30, 40, 50, and 100 μM DHC for 48 h inhibited the viability of MDA-MB-231 cells from 159.72 ± 9.87 to 103.58 ± 1.92 , 76.17 ± 11.71 , 75.06 ± 9.32 , 56.19 ± 6.03 , and 46.18 ± 7.74 , respectively (Fig. 1, lower image).

DHC inhibits cell proliferation and promotes apoptosis of MDA-MB-231 cells. The results of the EdU staining and flow cytometry both confirmed that DHC could effectively inhibit the proliferation of MDA-MB-231 cells. After treatment with 10, 50, and 100 μM DHC for 24 h, the percentages of the EdU-positive cells were significantly decreased (Fig. 2A and B). The cell proliferation percentage after 48 h of DHC treatment exhibited a similar trend to that observed for 24 h treatments (Fig. 2A and B). Flow cytometric assay also reinforced the results obtained through EdU staining assay. The number of MDA-MB-231 cells in the S-phase was markedly decreased, and the statistical results indicated that the percentage of cells in the S-phase was decreased from 32.87 ± 4.63 to 21.03 ± 3.81 ($P < 0.05$) (Fig. 2C). Furthermore, the effects of DHC on MDA-MB-231 cell apoptosis were detected utilizing flow cytometry. After treatment with 50 μM DHC for 48 h, the cell apoptosis rate was increased from 1.69 ± 0.83 to 21.17 ± 6.89 ($P < 0.05$) (Fig. 2D).

DHC inhibits the colony-forming activity and migration of MDA-MB-231 cells. The colony-forming activity of breast cancer cells could partially reflect the tumor malignancy. After treatment with 50 or 100 μM DHC for 12 days, the number of MDA-MB-231 colonies decreased from 233.43 ± 53.19 to 116.34 ± 31.08 ($P < 0.05$) and 69.17 ± 55.83 ($P < 0.05$), respectively (Fig. 3A). In addition, scratch assay results indicated that treatment with both 50 and 100 μM DHC decreased the migratory capacity of MDA-MB-231 cells, as the number of migratory cells was reduced from 152.42 ± 26.34 to 97.84 ± 13.02 ($P < 0.05$) and 66.34 ± 28.37 ($P < 0.05$), respectively (Fig. 3B).

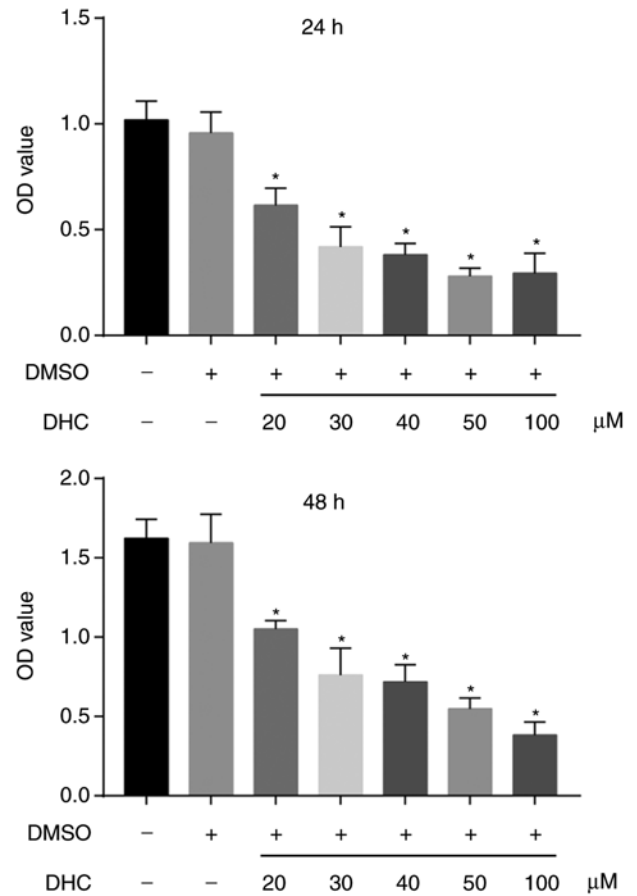


Figure 1. Cell viability is significantly inhibited by DHC in a dose-dependent manner at concentration ranging from 20 to 100 μM for 24 and 48 h. * $P < 0.05$ vs. DMSO only. DHC, dehydrocorydaline; OD, optical density.

DHC regulates the expression level of cell proliferation-, migration- and apoptosis-associated genes. The expression levels of genes involved in cell proliferation, migration and apoptosis was quantified after the treatment of MDA-MB-231 cells with DHC. Both *CDK1* and *CCND1* were critical proliferation-relevant genes, and both were significantly downregulated after treatment with 20 and 50 μM DHC for 48 h (Fig. 4A). Moreover, *MMP2* and *MMP9* play a key role in tumor metastasis through the degradation of the extra-cellular matrix. In this study, DHC also inhibited the expression of *MMP2* and *MMP9*, both at the mRNA and protein level (Fig. 4A, C and E). Furthermore, the mRNA levels of *caspases 3/8/9*, and the production of cleaved caspases 3/9 were analyzed. As revealed in Fig. 4B, 20 and 50 μM DHC treatment significantly increased the mRNA levels of *caspases 3/8/9* by 48.93 ($P < 0.05$) and 103.87 ($P < 0.05$), 97.83 ($P < 0.05$) and 147.64 ($P < 0.05$), 26.13 (no significant difference) and 97.47 ($P < 0.05$), respectively. Concerning the protein production levels, the levels of activated caspase-3 and caspase-9 were both decreased ($P < 0.05$; Fig. 4D and F).

DHC inhibits the growth of MDA-MB-231 tumor xenografts in SCID mice. The results obtained in this study revealed that DHC could reduce the tumor growth activity *in vivo*. After subcutaneous injection for 3 weeks, the newly formed tumor tissues were removed, photographed and weighed. The tumor volume was significantly reduced after DHC treatment

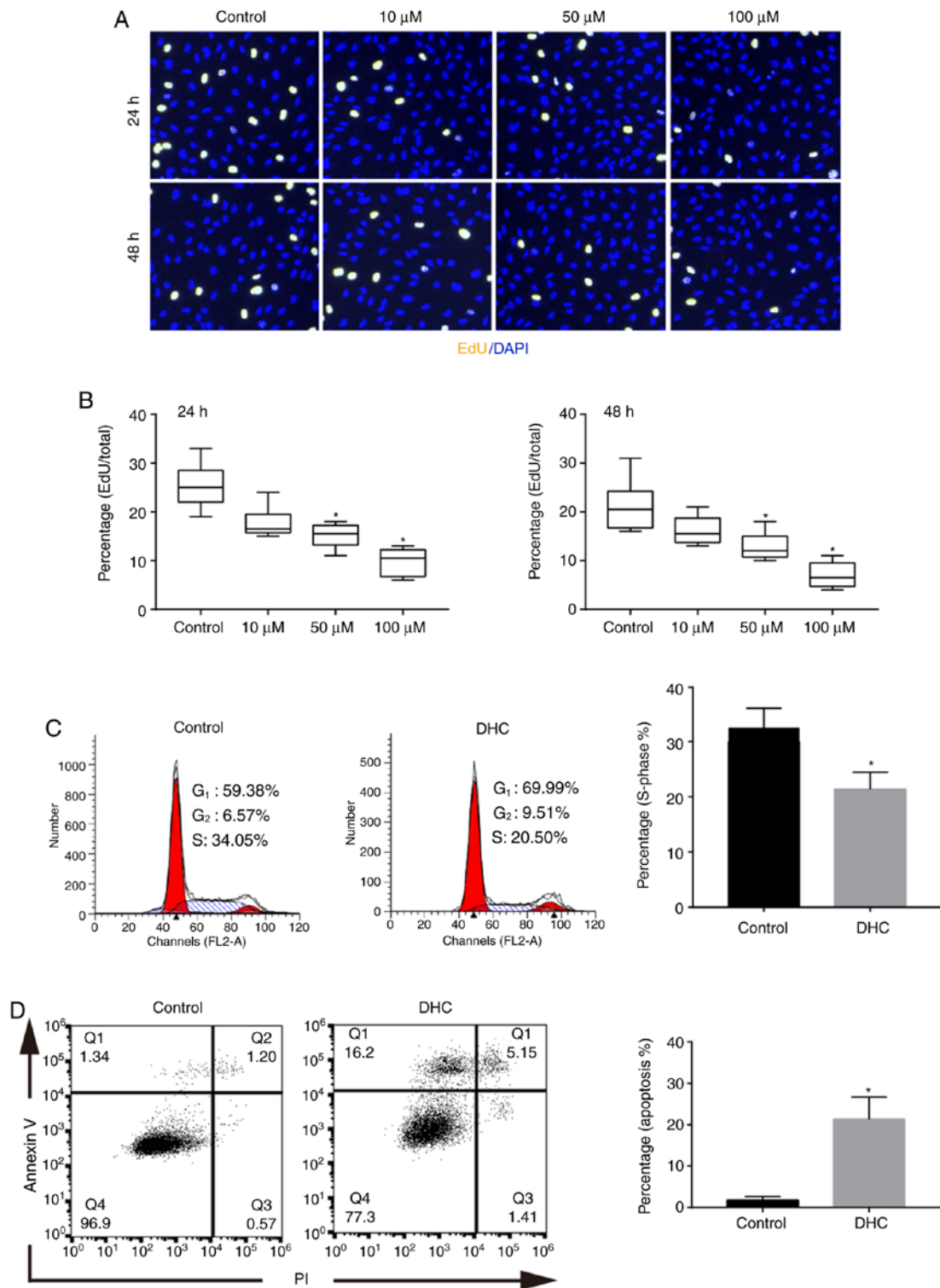


Figure 2. DHC inhibits the proliferation and induces the apoptosis of MDA-MB-231 cells. (A) EdU assay for DNA synthesis with DHC (10, 50, and 100 μ M) treatment for 24 and 48 h (magnification, x200). (B) Statistical comparison of EdU-positive count of DHC treatments vs. the control respectively. (C) Flow cytometric assay for cell cycle distribution with DHC (50 μ M) treatment for 48 h, and (D) flow cytometric assay for apoptosis with DHC (50 μ M) treatment for 48 h. * P <0.05 vs. the control group. DHC, dehydrocorydaline; EdU, 5-ethynyl-2'-deoxyuridine; PI, propidium iodide.

(Fig. 5A). In addition, the tumor weight also decreased from 1.78 ± 2.31 to 0.68 ± 0.28 g (P <0.05; Fig. 5B).

DHC inhibits cell proliferation in newly-formed tumor in vivo. The impact of DHC on the proliferation of MDA-MB-231 cells was detected through hematoxylin-eosin (H&E) staining,

and Ki67 and PCNA IHC. H&E staining revealed that the cell density was markedly reduced in DHC groups (Fig. 5C). Furthermore, the expression levels of Ki67 and PCNA were employed to evaluate cell proliferation alterations. In this study, continuous treatment with DHC limited cell proliferation in the newly formed tumors (Fig. 5C), therefore effectively

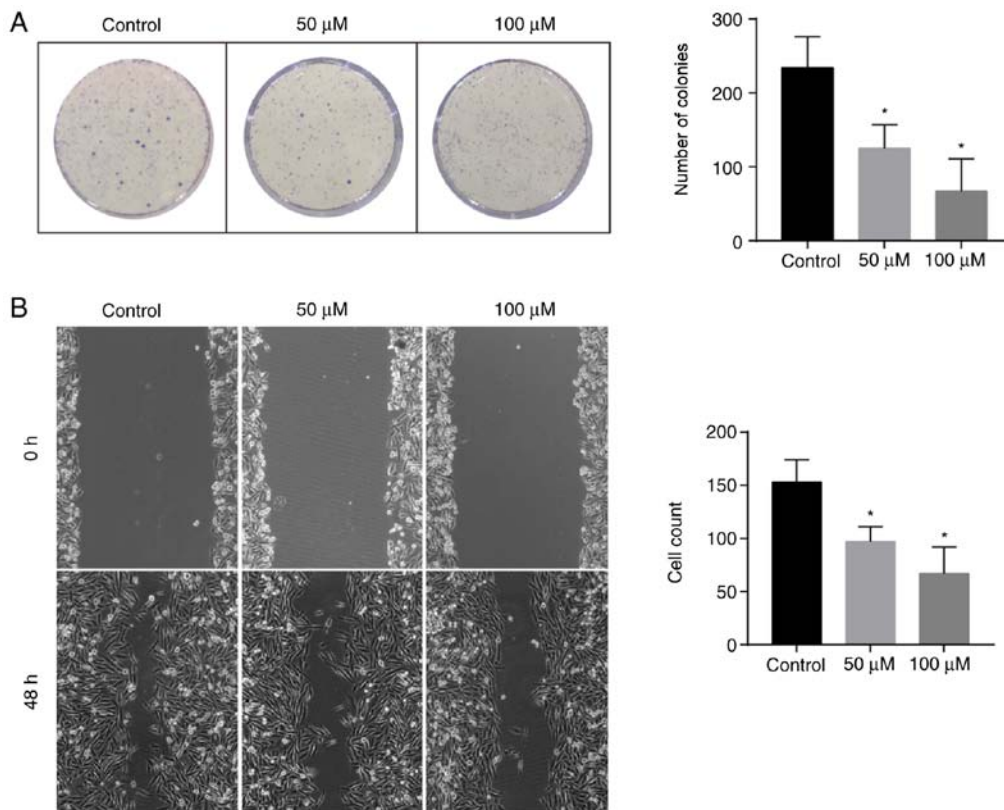


Figure 3. DHC treatments (50 and 100 μ M) inhibit colony formation and migration of MDA-MB-231 cells. (A) Colony formation was inhibited by DHC treatment for 12 days. Colonies containing ≥ 50 cells were counted for statistical comparison (magnification, $\times 100$) (B) Scratch assay for cell migration with or without DHC for 48 h (magnification, $\times 100$). * $P < 0.05$ vs. the control group. DHC, dehydrocorydaline.

hindering tumor progression. Ki67- and PCNA-positive cells were counted. The results revealed that Ki67- and PCNA-positive cell ratios were significantly decreased from 59.12 ± 5.32 to 26.47 ± 5.92 ($P < 0.05$) and from 48.36 ± 9.76 to 21.78 ± 9.83 ($P < 0.05$), respectively (Fig. 5D and E).

Discussion

DHC exhibits antitumor effects and plays an active role in inhibiting the proliferation and migration of cancer cells. For example, Huo *et al* (8) and other groups reported the effects of DHC on spinal bone cancer pain and microglia polarization, since it had been revealed that DHC could attenuate bone cancer pain. Lee *et al* (9) reported that DHC could decrease the migration capacity of non-small cell lung carcinoma cells. However, there are very few studies on the effects of DHC treatment in breast cancer. Considering that DHC certainly has cytotoxic activity, unraveling the mechanism of action through which DHC inhibits the proliferation and migration of breast cancer cells is of great interest for the clinical treatment of breast cancer.

A previous study (9) revealed that DHC impairs the migration of non-small cell lung carcinoma cells by downregulating MMP protein production, which is consistent with our findings. Our experimental results confirmed that DHC inhibited the expression of *MMP2* and *MMP9*, thereby inhibiting the metastasis of MDA-MB-231 cells. *MMP2* and *MMP9* are capable of degrading extracellular matrices, and play a key role during tumor metastasis. MMPs are a class of extracellular matrix-degrading enzymes that are considered to be

important enzymes for the degradation of the extracellular matrix and basement membrane (10). For instance, *MMP2* plays an important role in cell migration and tumor invasion (11), *MMP7* inhibits cell adhesion (12), and *MMP9* is a prerequisite for cell migration (13).

DHC-induced apoptosis may be the key activity granting its anticancer efficacy. The present results revealed that DHC treatment resulted in a significant decrease in the production of the anti-apoptotic protein *BCL2*, and an increase in the expression of the pro-apoptotic caspases 3/8/9. Flow cytometric results revealed that the percentage of apoptotic breast cancer cells increased after 48 h of treatment with 50 μ M DHC. Apoptosis-related proteins are classified into two types: An anti-apoptotic class (that prevents apoptosis) and a pro-apoptotic class (that induces apoptosis). *BCL2* family proteins are critical apoptosis-related proteins. Some authors have reported that *BCL2* overexpression blocks the effects of DHC on cell proliferation and migration, suggesting that *BCL2*-mediated anti-apoptotic activity could underlie the DHC anticancer activity. Inhibition of *BCL2* activates downstream caspase proteins and triggers cancer cell apoptosis (14). The present experimental results revealed that the effect of DHC treatment on proliferation-related proteins *CDK1* and *CCDN1* was consistent with the one exerted on *BCL2*.

Other studies have revealed that DHC inhibits the proliferation of MCF-7 cells by modulating the Bax/Bcl-2-mediated apoptosis and activating proteins belonging to the caspase family (15). This indicates that *BCL2*-mediated apoptosis plays an important role in the antitumor effect of DHC.

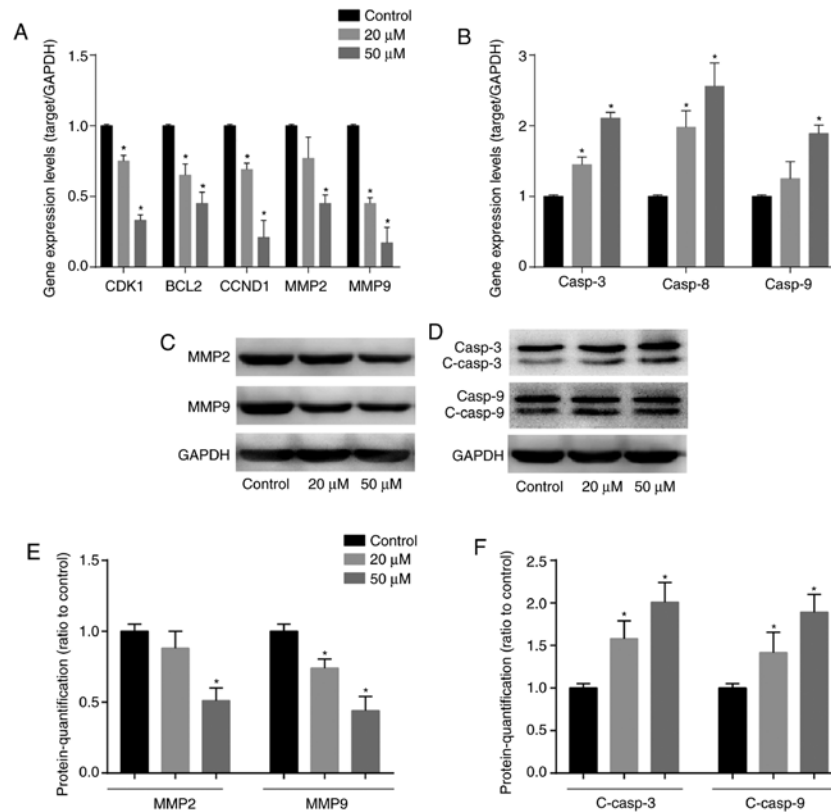


Figure 4. DHC affects the expression levels of oncogenes, apoptotic markers and MMPs. Reverse transcription-quantitative PCR was used to analyze the expression levels of (A) CDK1, BCL2, CCND1, MMP2, MMP9 and (B) caspase 3/8/9 of MDA-MB-231 cells treated with DHC (20 and 50 μ M) for 48 h. Western blotting was used to analyze the protein expression levels of (C) MMP2, MMP9 and (D) caspase 3, caspase 9, cleaved caspase 3 and cleaved caspase 9 in MDA-MB-231 cells treated with DHC (20 and 50 μ M) for 48 h. Quantification of the western blot analysis for the protein expression of (E) MMP2 and MMP9 and (F) cleaved caspase 3 and cleaved caspase 9. * P <0.05 vs. the control group. DHC, dehydrocorydaline; CDK1, cyclin-dependent kinases 1; CCND1, cyclin D1; MMP, matrix metalloproteinase; casp, caspase; c, cleaved.

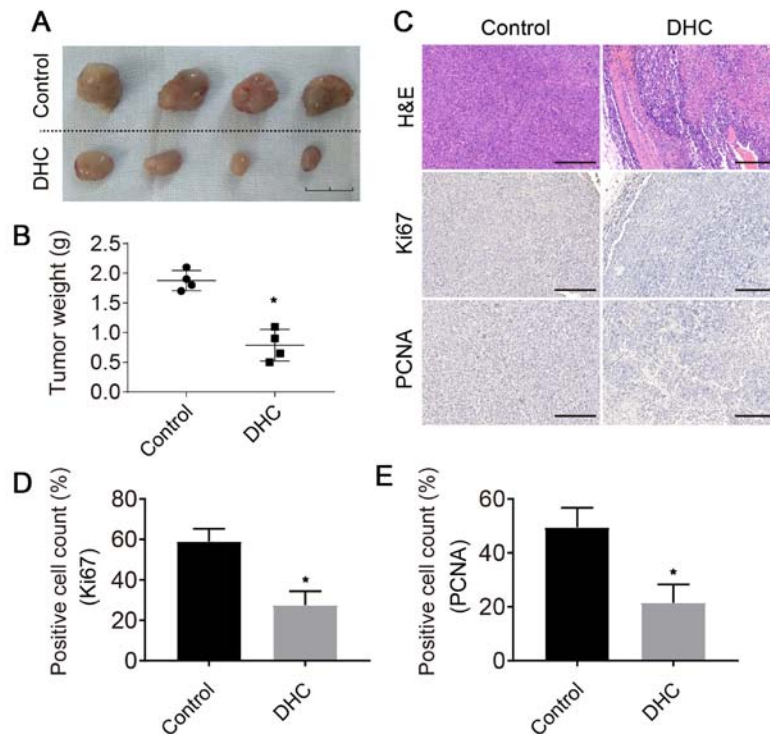


Figure 5. DHC inhibits breast cancer progression in a xenograft breast cancer nude mouse model for 3 weeks. (A) Macroscopic observation of implanted tumors with (DHC) or without (control) DHC treatments. Scale bar, 1 cm. (B) Statistical analysis of the tumor weight. (C) Immunohistochemical analysis and semi-quantification of (D) Ki67 and (E) PCNA expression. Scale bar, 100 μ m. * P <0.05 vs. the control group. DHC, dehydrocorydaline; IHC, immunohistochemical; PCNA, proliferating cell nuclear antigen.

Caspase family proteins play an important role in the induction, transduction, and amplification of intracellular apoptotic signaling (16). Caspase-8 and -10 are generally considered apoptotic activators in the exogenous pathway, while caspase-9 and -2 play important roles in the endogenous pathway, and Caspase-3 and -7 are the main effectors of apoptosis (10). Although DHC has the effect of inhibiting triple negative breast cancer cells MDA-MB-231, it is unknown whether DHC exerts inhibition on other types of human breast cancer cell lines such as SK-BR-3, BT-20 and MCF7. Therefore, in a follow-up study, comprehensive examination of the inhibitory effect of DHC on different types of breast cancer will be performed.

In conclusion, DHC was revealed to inhibit the migration and proliferation of MDA-MB-231 cells. In addition, DHC also promoted the apoptosis of breast cancer cells by inhibiting the production of BCL2 and upregulating the expression of caspases. *In vivo* experiments confirmed that DHC could further slow tumor progression by restricting angiogenesis at this level. The present results indicated that DHC is a promising drug candidate for breast cancer treatment.

Acknowledgements

Not applicable.

Funding

The present study was supported by the Research project of Wuhan health and family planning commission, 2014 (project leader, YH; grant no. WX14D04).

Availability of data and materials

The datasets used and/or analyzed during the present study are available from the corresponding author on reasonable request.

Authors' contributions

YH and GZ conceived and designed the study. YH and HH analyzed the data, and wrote and revised the manuscript. SW and FC analyzed and interpreted the data. GZ provided financial support, and wrote and revised the manuscript. All authors read and approved the final manuscript.

Ethics approval and consent to participate

The present study was approved by the Fifth Hospital of Wuhan.

Patient consent for publication

Not applicable.

Competing interests

The authors declare that they have no competing interests.

References

1. Park Y, Shackney S and Schwartz R: Network-based inference of cancer progression from microarray data. *IEEE/ACM Trans Comput Biol Bioinforma* 6: 200-212, 2009.
2. Ghoncheh M, Pournamdar Z and Salehiniya H: Incidence and mortality and epidemiology of breast cancer in the world. *Asian Pac J Cancer Prev* 17: 43-46, 2016.
3. Mukherjee AK, Basu S, Sarkar N and Ghosh AC: Advances in cancer therapy with plant based natural products. *Curr Med Chem* 8: 1467-1486, 2001.
4. Sun Y, Xun K, Wang Y and Chen X: A systematic review of the anticancer properties of berberine, a natural product from Chinese herbs. *Anticancer Drugs* 20: 757-769, 2009.
5. Xu Z, Chen X, Fu S, Bao J, Dang Y, Huang M, Chen L and Wang Y: Dehydrocorydaline inhibits breast cancer cells proliferation by inducing apoptosis in MCF-7 cells. *Am J Chin Med* 40: 177-185, 2012.
6. Masood A, Azmi AS and Mohammad RM: Small molecule inhibitors of Bcl-2 family proteins for pancreatic cancer therapy. *Cancers (Basel)* 3: 1527-1549, 2011.
7. Livak KJ and Schmittgen TD: Analysis of relative gene expression data using real-time quantitative PCR and the 2(-Delta Delta C(T)) method. *Methods* 25: 402-408, 2001.
8. Huo W, Zhang Y, Liu Y, Lei Y, Sun R, Zhang W, Huang Y, Mao Y, Wang C, Ma Z and Gu X: Dehydrocorydaline attenuates bone cancer pain by shifting microglial M1/M2 polarization toward the M2 phenotype. *Mol Pain* 14: 1744806918781733, 2018.
9. Lee J, Sohn EJ, Yoon SW, Kim CG, Lee S, Kim JY, Baek N and Kim SH: Anti-metastatic effect of dehydrocorydaline on H1299 non-small cell lung carcinoma cells via inhibition of matrix metalloproteinases and B cell lymphoma 2. *Phyther Res* 31: 441-448, 2017.
10. Lu P, Takai K, Weaver VM and Werb Z: Extracellular Matrix degradation and remodeling in development and disease. *Cold Spring Harb Perspect Biol* 3: pii: a005058, 2011.
11. Fromigué O, Hamidouche Z and Marie PJ: Blockade of the RhoA-JNK-c-Jun-MMP2 cascade by atorvastatin reduces osteosarcoma cell invasion. *J Biol Chem* 283: 30549-30556, 2008.
12. Basu S, Thorat R and Dalal SN: MMP7 is required to mediate cell invasion and tumor formation upon plakophilin3 loss. *PLoS One* 10: e0123979, 2015.
13. Dufour A, Zucker S, Sampson NS, Kuscu C and Cao J: Role of matrix metalloproteinase-9 dimers in cell migration: Design of inhibitory peptides. *J Biol Chem* 285: 35944-35956, 2010.
14. Li WH, Wu HJ, Li YX, Pan HG, Meng T and Wang X: MicroRNA-143 promotes apoptosis of osteosarcoma cells by caspase-3 activation via targeting Bcl-2. *Biomed Pharmacother* 80: 8-15, 2016.
15. Dolka I, Król M and Sapiernyński R: Evaluation of apoptosis-associated protein (Bcl-2, Bax, cleaved caspase-3 and p53) expression in canine mammary tumors: An immunohistochemical and prognostic study. *Res Vet Sci* 105: 124-133, 2016.
16. Galluzzi L, Bravo-San Pedro JM and Kroemer G: Ferroptosis in p53-dependent oncosuppression and organismal homeostasis. *Cell Death Differ* 22: 1237-1238, 2015.



This work is licensed under a Creative Commons Attribution-NonCommercial-NoDerivatives 4.0 International (CC BY-NC-ND 4.0) License.